

See discussions, stats, and author profiles for this publication at: <https://www.researchgate.net/publication/23714659>

In Situ Analysis of a Bimodal Size Distribution of Superparamagnetic Nanoparticles

ARTICLE in ANALYTICAL CHEMISTRY · FEBRUARY 2009

Impact Factor: 5.64 · DOI: 10.1021/ac802009q · Source: PubMed

CITATIONS

27

READS

81

4 AUTHORS, INCLUDING:



Andreas F Thünemann

Bundesanstalt für Materialforschung und -...

178 PUBLICATIONS 4,966 CITATIONS

SEE PROFILE



Patrick Knappe

Currently searching for a job opportunity i...

14 PUBLICATIONS 100 CITATIONS

SEE PROFILE



Steffen Weidner

Bundesanstalt für Materialforschung und -...

94 PUBLICATIONS 1,294 CITATIONS

SEE PROFILE

In Situ Analysis of a Bimodal Size Distribution of Superparamagnetic Nanoparticles

Andreas F. Thünemann,* Simone Rolf, Patrick Knappe, and Steffen Weidner

BAM Federal Institute for Materials Research and Testing, Richard-Willstätter-Straße 11, 12489 Berlin, Germany

The dispersed iron oxide nanoparticles of ferrofluids in aqueous solution are difficult to characterize due to their protective polymer coatings. We report on the bimodal size distribution of superparamagnetic iron oxide nanoparticles found in the MRI contrast agent Resovist, which is a representative example of commercial nanoparticle-based pharmaceutical formulations. The radii of the majority of the nanoparticles (>99%) range from 4 to 13 nm (less than 1% of the particles display radii up to 21 nm). The maxima of the size distributions are at 5.0 and 9.9 nm. The analysis was performed with in situ characterization of Resovist via online coupling of asymmetrical flow field-flow fractionation (A4F) with small-angle X-ray scattering (SAXS) using a standard copper X-ray tube as a radiation source. The outlet of the A4F was directly coupled to a flow capillary on the SAXS instrument. SAXS curves of nanoparticle fractions were recorded at 1-min time intervals. We recommend using the A4F-SAXS coupling as a routine method for analysis of dispersed nanoparticles with sizes in the range of 1–100 nm. It allows a fast and quantitative comparison of different batches without the need for sample preparation.

INTRODUCTION

Nanoparticle dispersions are of tremendous importance in many fields of nanotechnology, especially in the development of pharmaceutical applications, such as target-specific drug delivery,¹ gene therapy,^{2,3} and cancer diagnosis.^{4,5} Nanoparticles are of similar importance in the classical field of colloid and polymer science; for example, polymer latexes and ferrofluids. Along with their benefits, serious concerns have also arisen about safety risks of nanoparticles to human health and the environment.^{6–9} It is therefore of utmost importance to implement sustainable and

reliable analytical methods in nanoparticle characterizations. Detailed knowledge of nanoparticle size, shape, number, composition, and structure is needed, since there is no doubt that these quantities determine efficiency in technical applications as well as their risk potential. For a systematic optimization of the desired nanoparticles and the quantitative characterization of different production batches, it is necessary to have rapid and precise analytical methods for particle size and shape determination. Such procedures are not yet available for broad size distributions or polydisperse samples.

In addition to the predominant particle size determination techniques (electron microscopy and dynamic light scattering), one currently observes a renaissance of classical methods, such as analytical ultracentrifugation and small-angle X-ray scattering (SAXS). The latter is a state-of-the-art method for the determination of nanoparticle size, shape, number, and inner structure of nanoparticles in solution without the need for sample preparation steps.^{10–13} However, SAXS data interpretation is ambiguous if the nanoparticles are polydisperse or if they differ in shape. This is due to the fact that SAXS averages the scattering pattern of all particles in the sample. In short, SAXS is normally very accurate if all particles are of similar size and shape. Therefore, fractionation of particle mixtures before performing SAXS is necessary for unambiguous results.

The A4F method is appropriate for gentle fractionation because it applies lower shear forces to the particles than GPC and HPLC. The sizes of the particles in the fractions can then be determined online with multiangle light scattering (MALS). For example, A4F-MALS systems are successfully used in the analysis of gelatin nanoparticle drug carriers,¹⁴ polyorganosiloxane nanoparticles,¹⁵ and chitosan.¹⁶

Surprisingly, SAXS has not previously been combined with field-flow fractionation methods. This is most probably due to the fact that scattering of visible light by nanoparticles is several orders

* Corresponding author. E-mail: andreas.thuenemann@bam.de.

- (1) Solaro, R. J. *Polym. Sci., Part A* **2008**, *46*, 1–11.
- (2) Weiss, S. I.; Sieverling, N.; Niclasen, M.; Maucksch, C.; Thünemann, A. F.; Mohwald, H.; Reinhardt, D.; Rosenecker, J.; Rudolph, C. *Biomaterials* **2006**, *27*, 2302–2312.
- (3) Rudolph, C.; Sieverling, N.; Schillinger, U.; Lesina, E.; Plank, C.; Thünemann, A. F.; Schonberger, H.; Rosenecker, J. *Biomaterials* **2007**, *28*, 1900–1911.
- (4) Ferrari, M. *Nat. Rev. Cancer* **2005**, *5*, 161–171.
- (5) Jain, P. K.; El-Sayed, I. H.; El-Sayed, M. A. *Nano Today* **2007**, *2*, 18–29.
- (6) Tsuji, J. S.; Maynard, A. D.; Howard, P. C.; James, J. T.; Lam, C. W.; Warheit, D. B.; Santamaria, A. B. *Toxicol. Sci.* **2006**, *89*, 42–50.
- (7) Maynard, A. D.; Aitken, R. J.; Butz, T.; Colvin, V.; Donaldson, K.; Oberdorster, G.; Philbert, M. A.; Ryan, J.; Seaton, A.; Stone, V.; Tinkle, S. S.; Tran, L.; Walker, N. J.; Warheit, D. B. *Nature* **2006**, *444*, 267–269.
- (8) Maynard, A. D. *Ann. Occup. Hyg.* **2007**, *51*, 1–12.

- (9) Balbus, J. M.; Maynard, A. D.; Colvin, V. L.; Castranova, V.; Daston, G. P.; Denison, R. A.; Dreher, K. L.; Goering, P. L.; Goldberg, A. M.; Kulinowski, K. M.; Monteiro-Riviere, N. A.; Oberdorster, G.; Omenn, G. S.; Pinkerton, K. E.; Ramos, K. S.; Rest, K. M.; Sass, J. B.; Silbergeld, E. K.; Wong, B. A. *Environ. Health Perspect.* **2007**, *115*, 1654–1659.
- (10) Glatter, O.; Kratky, O. *Small Angle X-ray Scattering*; Academic Press: London, 1982.
- (11) Fritz, G.; Glatter, O. *J. Phys. Condens. Matter* **2006**, *18*, S2403–S2419.
- (12) Konarev, P. V.; Petoukhov, M. V.; Volkov, V. V.; Svergun, D. I. *J. Appl. Crystallogr.* **2006**, *39*, 277–286.
- (13) Svergun, D. I. *J. Appl. Crystallogr.* **2007**, *40*, S10–S17.
- (14) Fraunhofer, W.; Winter, G.; Coester, C. *Anal. Chem.* **2004**, *76*, 1909–1920.
- (15) Jungmann, N.; Schmidt, M.; Maskos, M. *Macromolecules* **2001**, *34*, 8347–8353.
- (16) Mao, S.; Augsten, C.; Mader, K.; Kissel, T. J. *Pharm. Biomed. Anal.* **2007**, *45*, 736–741.

of magnitude higher than that of X-rays. A priori, one can expect that the SAXS signal of the nanoparticles after field-flow fractionation will be too low to be detected. In a recent study, we circumvented this problem by using a highly intense X-ray source in the form of synchrotron radiation in combination with a SAXS system optimized for nanoparticle detection.¹⁷ It has been shown that the size distribution of the radii (1.2–1.7 nm) and lengths (7.0–30.0 nm) of superparamagnetic maghemite nanorods can be revealed in situ by the A4F-SAXS coupling. Unfortunately, synchrotron X-ray radiation is not readily available for routine work; for example, for the control of different production batches. Therefore, this study's objective is to show that an A4F-SAXS coupling is also possible with reasonable resolution when using a commercial X-ray source. The time-saving determination of the size distributions of superparamagnetic nanoparticles (Resovist) for medical use, whose particle size distribution cannot be determined with other methods, such as TEM¹⁸ and DLS, is demonstrated.

MATERIALS AND METHODS

Materials. The commercial magnetic resonance imaging contrast agent Resovist was purchased from Bayer-Schering AG. Resovist is an aqueous suspension of superparamagnetic iron oxide nanoparticles coated with carboxydextran.¹⁹ It contains 540 mg/mL Ferucarbotran, corresponding to 28 mg/mL of iron. NovaChem Surfactant 100 was obtained from Postnova Analytics GmbH, Germany. This surfactant mixture is also available as FL-70 from Fischer Scientific (USA). For use in chromatography and composition, see ref 20.

Methods. *Asymmetrical Flow Field-Flow Fractionation (A4F).* The A4F unit was from Postnova Analytics GmbH (Germany), and consisted of an AF2000 focus system (PN 5200 sample injector, PN 7505 inline degaser, PN 1122 tip, and focus pump). An inline solvent filter (100 nm, regenerated cellulose, Postnova) was placed between the solvent pumps (between tip and focus) and the channel to reduce the background signals. The channel thickness was 500 μm , and the ultra filtration membrane was a regenerated cellulose membrane with a cutoff of $10 \times 10^3 \text{ g mol}^{-1}$. The solvent used was water containing 0.2% (v/v) NovaChem Surfactant 100. The detector flow rate was 0.5 mL min^{-1} for all A4F experiments, and the cross-flow rate was controlled by AF2000 software (Postnova Analytics). The cross-flow decreased linearly with time, starting with a cross-flow of 2.5 mL min^{-1} and decreasing at a rate of $2.5/20 \text{ mL min}^{-2}$. A sample of nanoparticles (Resovist) with a concentration of 7.1 mg/mL of iron (10.0 mg/mL of maghemite) and a volume of $50 \mu\text{L}$ was injected into the channel for each experiment; that is, a total of $355 \mu\text{g}$ of iron ($507 \mu\text{g}$ of maghemite). The outlet of the A4F was coupled directly to the UV detector (detection at $\lambda = 300 \text{ nm}$) and the flow cell of the SAXS instrument. The fractionated stream reached the UV detector approximately 1 min after passing through the flow cell of the SAXS instrument.

SAXS. SAXS measurements were performed with a Kratky-type instrument (SAXSess from Anton Paar, Austria) at $20 \pm 1^\circ\text{C}$. The SAXSess has a low sample-to-detector distance (0.309 m), which is suitable for investigation of dispersions with low scattering intensities. The measured intensity was corrected by subtracting the intensity of a capillary filled with pure water. The scattering vector is defined in terms of the scattering angle θ and the wavelength λ of the radiation ($\lambda = 0.154 \text{ nm}$): thus, $q = 4\pi/\lambda \sin \theta$. Deconvolution (slit length desmearing) of the SAXS curves was performed with the SAXS-Quant software (version 2.0) from Anton Paar (Austria). In addition, the deconvolution was also performed with Glatter's established indirect Fourier transformation method^{10,11,21} implemented in the PCG Software Version 2.02.05 (University of Graz) to verify the results produced with the SAXS-Quant software.

The deconvoluted SAXS curves were analyzed by comparison with scattering model functions implemented in an IGOR Pro-based software package from NIST.²² Fractions of nanoparticles with index i are approximated by Gaussian distributions

$$f_i(R) = \frac{1}{\sigma_i \sqrt{2\pi}} \exp \left[-\frac{(R - R_i)^2}{2\sigma_i^2} \right] \quad (1)$$

where R_i is the average radius and σ_i is the width of the distribution. The polydispersity is defined as $p_i = \sigma_i/R_i$. The scattering of the distribution of spheres in a fraction with index i is

$$I_i(q) = k \frac{\phi_i}{\langle V_i \rangle} (\rho - \rho_s)^2 \int_0^\infty f_i(R) R^6 [F(qR)]^2 dR \quad (2)$$

Here, k is an instrumental constant, ϕ_i is the volume fraction of the particles, and $\rho - \rho_s$ the electron density difference between particles and solvent. The average volume of the particles in a fraction is $\langle V_i \rangle = 4/3\pi \langle R_i \rangle^3 = 4/3\pi R_i^3 (1 + 3p_i^2)$, and the scattering amplitude of a sphere is $F(qR) = (qR)^{-3} [\sin(qR) - qR \cos(qR)]$.

Dynamic Light Scattering (DLS). The DLS measurements were performed using a Malvern Instruments particle sizer (Zetasizer Nano ZS, Malvern Instruments, UK) equipped with a He–Ne laser ($\lambda = 632.8 \text{ nm}$). The scattering data were recorded at $20 \pm 1^\circ\text{C}$ in backscattering modus at a scattering angle of $2\theta = 173^\circ$, which corresponded to a scattering vector of $q = 4\pi n/\lambda \sin \theta$ (0.02636 nm^{-1}). The aqueous sample solutions were placed into a square $10 \times 10 \text{ mm}$ disposable polystyrene cuvette. Prior to measurement, the samples were filtered with a $0.45 \mu\text{m}$ Millipore syringe filter to remove dust particles. The hydrodynamic radius, R_h (of a hydrodynamic equivalent sphere), was obtained from the diffusion coefficient using the Stokes–Einstein relation, $R_h = kT/(6\pi\eta D)$.

RESULTS AND DISCUSSION

Dispersions of superparamagnetic iron oxide nanoparticles form ferrofluids²³ and have been widely used as a diagnostic agent for magnetic resonance imaging.¹⁹ The synthetic nanoparticles

(17) Thunemann, A. F.; Kegel, J.; Polte, J.; Emmerling, F. *Anal. Chem.* **2008**, *80*, 5905–5911.

(18) Wang, Y.; Ng, Y. W.; Chen, Y.; Shuter, B.; Yi, J.; Ding, J.; Wang, S. C.; Feng, S. S. *Adv. Funct. Mater.* **2008**, *18*, 308–318.

(19) Lawaczeck, R.; Menzel, M.; Pietsch, H. *Appl. Organomet. Chem.* **2004**, *18*, 506–513.

(20) Atta, K. R.; Gavril, D.; Loukopoulos, V.; Karaiskakis, G. *J. Chromatogr., A* **2004**, *1023*, 287–296.

(21) Glatter, O. J. *Appl. Crystallogr.* **1977**, *10*, 415–421.

(22) Kline, S. R. *J. Appl. Crystallogr.* **2006**, *39*, 895–900.

(23) Holm, C.; Weis, J. J. *Curr. Opin. Colloid Interface Sci.* **2005**, *10*, 133–140.

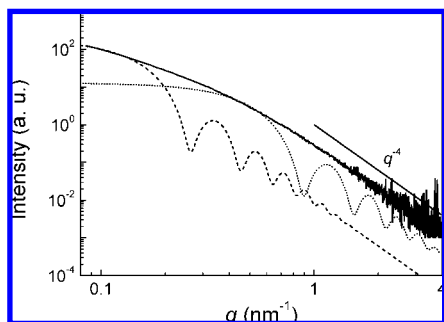


Figure 1. Experimental SAXS curve of nonfractionated Resovist nanoparticles (solid line) and simulated curves from particles with radii of 17 and 5 nm (dashed and dotted line). Polydispersity is 0.05. The Porod region ($1 < q < 4 \text{ nm}^{-1}$) is indicated by a straight line.

contain magnetite (Fe_3O_4), maghemite ($\gamma\text{-Fe}_2\text{O}_3$), or both.²⁴ Primary particle sizes in the range of 6–15 nm are assumed to be the optimum for MRI applications.²⁵ All superparamagnetic contrast agents contain nanoparticles, which are typically coated with large quantities of polymers, such as dextran, carboxydextran, starch, silicones, albumin, or polyethylene oxide (PEO, polyethylene glycol, PEG) for colloidal stability. Examples for clinical used nanoparticles are products under the trade names Lumirem (radius, $R_h = 150 \text{ nm}$), Endorem ($R_h = 40\text{--}75 \text{ nm}$), Sinerem ($R_h = 10\text{--}20 \text{ nm}$), and Resovist ($R_h = 30 \text{ nm}$).²⁶ Surprisingly, little data has been published on the size distributions of the nanoparticles, probably because these type of particles produce highly different results when different analytical methods are applied. As an example, the radii of the primary iron oxide nanoparticles of Resovist are roughly 2.5 nm as deduced from TEM pictures.¹⁸ This is much smaller than the hydrodynamic radius of Resovist nanoparticles (30 nm).¹⁸ The difference between 2.5 and 30 nm is attributed simply to the carboxydextran coating¹⁸ or resulting from carboxydextran-coated aggregates of multiple primary particles.²⁶ One may assume that the carboxydextran, which is surface-active to the nanoparticles, camouflages the TEM pictures by inducing diffuse aggregates.¹⁸ This is in agreement with the literature, where it has been reported that surface-active compounds can produce strong artifacts in TEM pictures of nanoparticles.²⁷ Therefore, TEM alone is not sufficient for the determination of the particle size distribution. In this context, SAXS could provide valuable information to solve this problem.

Size Determination of Nonfractionated Nanoparticles. The SAXS pattern of Resovist was therefore measured in situ without sample preparation. The resulting scattering is displayed in Figure 1 (solid line). It can be seen that the nanoparticles produce a strong signal where the scattering intensity scales with q^{-4} in the range of $1 < q < 4 \text{ nm}^{-1}$. This is in accordance with Porod's law, which reveals that the density transition between a particle

and its surroundings is sharp (absence of fractal structures).²⁸ Furthermore, the polymer coating is invisible for SAXS in the presence of iron oxide, as expected from the very low electron density difference between carboxydextran and water, as compared to that of iron oxide and water. A reasonable method for shape and size determination of nanoparticles from SAXS data is the direct fitting of model curves to experimental scattering curves. A detailed review is given by Pedersen.²⁹ The scattering intensity from noninteracting individual particles is determined by their form factor. We attempted to tentatively interpret the scattering by fitting the SAXS curve to the scattering from different particle sizes with varying size distributions and shapes. As expected, we were not able to fit the curve using reasonably simple models. Nevertheless, if we assume spherical particles, we can estimate that the largest particles have radii of approximately 17 nm and that the radii of the smallest are roughly 5 nm (compare the dashed and dotted lines, respectively, in Figure 1). In it, we used Gaussian size distributions with a fixed polydispersity of 0.05 for reasons of simplicity. The use of very broad size distributions did not provide any meaningful information. A bimodal size distribution of superparamagnetic nanoparticles is indicated by the measured SAXS curve, but without additional, more detailed information, it is clear that this assumption is highly speculative. To improve the analytical situation, we performed a detailed analysis by coupling A4F particle fractionation with SAXS shape analysis.

Nanoparticle Sizes from Online Fractionation. The nanoparticle analysis by A4F-SAXS coupling is based on the strategy that the fractionation process of the A4F provides nanoparticles with a narrow polydispersity ideal for SAXS analysis (performed online with the help of a flow cell). A sketch of the experimental setup is shown in Figure 2. In addition, a UV detector is positioned between the A4F and SAXS. We found that a linear decrease in the A4F cross-flow between separation times of 0 and 1200 s results in an optimum of nanoparticle separation, as indicated by the UV detector's signal (time-dependent cross-flow and UV-signal intensity are displayed in Figure 3). It can be seen that the first (smallest) nanoparticles are detected at a separation time of 270 s. Distinct maxima of the UV signal are at 490 and 1380 s, with a minimum at 900 s. The last (largest) nanoparticles which were eluted are detected around 1800 s, and no signal is subsequently observed.

A A4F-SAXS setup similar to that in Figure 2 was implemented recently at a synchrotron (BESSY), which allows the monitoring of SAXS curves of iron oxide nanorods at time intervals of one second or less.¹⁷ Instead of a synchrotron, the source of radiation in the present work is a commercial copper X-ray tube. This has a priori the consequence that the time required for recording a single SAXS curve of comparable data statistics increases by 2–3 orders of magnitude. Indeed, we found that SAXS data of reasonable quality can be recorded for Resovist at 60–120 s sampling time intervals when using the same injection volume and iron oxide concentration (see the Materials and Methods Section), as in the A4F-SAXS synchrotron study.¹⁷ Typical SAXS curves at three different fractionation times (300, 540, and 1500 s)

(24) Thunemann, A. F.; Schutt, D.; Kaufner, L.; Pison, U.; Mohwald, H. *Langmuir* **2006**, *22*, 2351–2357.

(25) Chatterjee, J.; Haik, Y.; Chen, C. J. *J. Magn. Magn. Mater.* **2003**, *257*, 113–118.

(26) Wang, Y. X. J.; Hussain, S. M.; Krestin, G. P. *Eur. Radiol.* **2001**, *11*, 2319–2331.

(27) Kreuter, J. *Int. J. Pharm.* **1983**, *14*, 43–58.

(28) Ruland, W. *Carbon* **2001**, *39*, 323–324.

(29) Pedersen, J. S. *Adv. Colloid Interface Sci.* **1997**, *70*, 171–210.

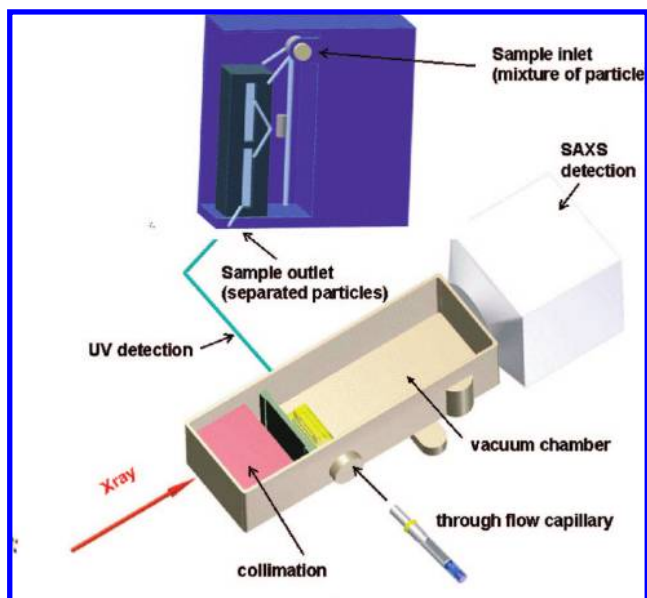


Figure 2. Sketch of the experimental setup of the A4F (top) and SAXS (bottom) coupling. Particle fractionation is performed in the A4F. Particles leave the outlet of the A4F consecutively as small, medium-sized, and large particles. The stream of the fractionated particles is first detected by UV absorption at 300 nm and 1 min later in a flow cell by SAXS (shortest possible detection time interval is 60 s).

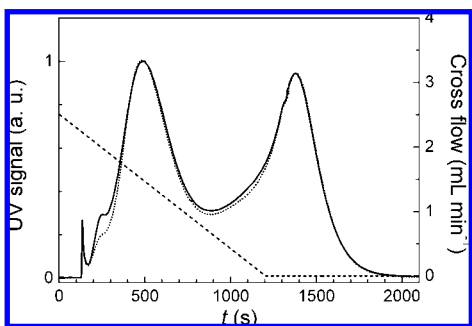


Figure 3. Fractograms of the asymmetrical field-flow fractionation of Resovist samples with UV detection at 300 nm for two experiments (solid and dotted line). The maximum of the first peak is normalized to one. A linear decay of the cross-flow rate from 2.5 mL min⁻¹ to zero was applied in the range from 0 to 1200 s (dashed line); no cross-flow was applied thereafter. The flow rate was constant with 0.5 mL min⁻¹.

are displayed in Figure 4 (solid gray lines). Note that the particles are already diluted when injected into the A4F (iron content 7.1 g/L, nonfractionated) and further diluted by a factor of about 100 during fractionation. In contrast to the nonfractionated Resovist (Figure 1), the shape of the curves of the fractionated particles is typical for spherical particles.²⁹ For a quantitative description, we used the model of polydisperse spheres with a Gaussian distribution as given by eq 2. Examples of best fit curves with particle radii of 4.7, 6.9, and 13.8 nm are given in Figure 4 (black solid lines). The polydispersities were held constant at a value of 0.05 for all fits to avoid ambiguous results. The radii and their uncertainty values from the curve fittings (error bars) are summarized as a function of the fractionation time in Figure 5. It can be seen that the first particles with radii of 5 nm were detected at a fractionation time of 300 s and the last with radii of 19 nm, at 1740 s, which is in agreement with the first and last particle

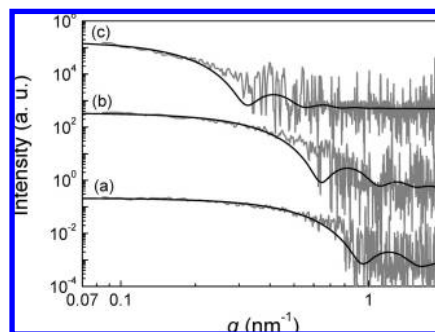


Figure 4. Experimental SAXS pattern of nanoparticle fractions collected at retention times of 300, 540, and 1500 s (solid gray lines, a–c). The fit curves (black solid curves) correspond to spherical particles with radii of 4.7 nm (a), 6.9 nm (b), and 13.8 nm (c) of Gaussian particle size distributions with a polydispersity of 0.05. Intensities are multiplied by a factor of 10² (b) and 10⁴ (c) for clarity of presentation. The radii are fit parameters but not the polydispersities, which are constant at a value of 0.05, to avoid ambiguous fit results.

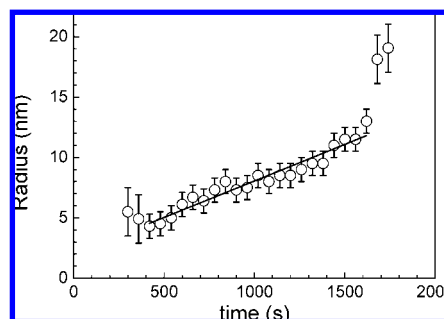


Figure 5. The mean radii of the nanoparticles as a function of the A4F fractionation time (circles). The increase in the radii with elution time is approximated as a linear function in the interval from 400 to 1600 s.

detection times from UV. The values of the radii of the smallest and largest particles are close to those derived from the nonfractionated samples.

The increase in the radii with fractionation time can be approximated by a linear function as $R(t) = 1.99 \text{ nm} + (6.06 \times 10^{-3} \text{ nm s}^{-1})t$ for times between 400 and 1600 s (solid line in Figure 5). This linear increase is in accordance with the theoretical prediction of A4F separation of spherical particles.^{14,30} Note that the two first and last data values are not used for approximation because of the very low SAXS intensities of the fractions at the shortest and largest fractionation times.

Bimodal Size Distribution. The quantitative determination of the size distribution, which is bimodal, as seen in the UV trace, is of great interest. Unfortunately, the UV signal intensity of the nanoparticles (Figure 3) allows no quantitative frequency scaling of the radii (Figure 5) for determination of their size distribution (Lambert–Beer's law is not valid for particles). The necessary information is given by the scaling factor of the SAXS intensity fits, which is directly proportional to the volume fraction of the nanoparticles (cf. eq 2). The resulting volume-weighted frequency of the particles as a function of their radii is displayed in Figure

(30) Thielking, H.; Roessner, D.; Kulicke, W. M. *Anal. Chem.* **1995**, *67*, 3229–3233.

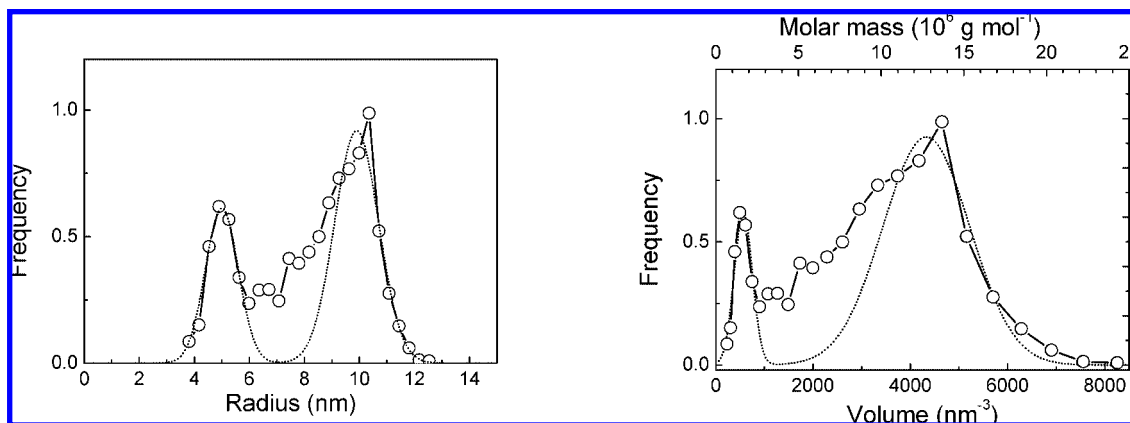


Figure 6. (Left) Volume-weighted frequency distribution of the nanoparticles as a function of their radii (circles). A sum of two Gaussian distributions with maxima at $R = 5.0$ and 9.9 nm with width of $\sigma = 1.2$ and 1.6 nm were used for approximation (dotted line). The radii-weighted ratio of small to large particles is 1:2. (Right) Frequency distribution of the nanoparticles as a function of their volumes (lower x -axis) and their molar mass (upper x -axis). The volume-weighted ratio of small to large particles is 1:7.

6. An approximation by two Gaussian distributions has maxima at $R = 5.0$ and 9.9 nm with widths of $\sigma = 1.2$ and 1.6 nm, respectively (solid line in Figure 6). As can be seen, the frequency ratio of the smaller to larger nanoparticles is about 1:2. It can be further seen that the majority of the particles ($>99\%$) are in a range between 4 and 13 nm. A small quantity ($<1\%$) of larger particles with radii up to 21 nm was detected after lengthy elution. Due to the fact that the scattering intensity scales with R^6 , SAXS is very sensitive to larger particles (see eq 2), even in very small concentration regimes. In addition to the radii, the volume and molar mass distribution can be determined (Figure 6, right figure). The latter is calculated by multiplying the nanoparticles' volumes by the bulk density of maghemite (4.89 g cm^{-3}) and Avogadro's number (upper x -axis). It can be seen that the smallest nanoparticles have a volume of 230 nm^3 , which contains approximately 8500 iron atoms and a molar mass of $M = 0.68 \times 10^6 \text{ g mol}^{-1}$. The largest particles have a volume of 8260 nm^3 (3.0×10^5 iron atoms, $M = 24.3 \times 10^6 \text{ g mol}^{-1}$). The bimodality of the size distribution, which is approximated by two Gaussian distributions (dotted line) with maxima at volumes of 566 nm^3 ($M = 1.7 \times 10^6 \text{ g mol}^{-1}$) and 4330 nm^3 ($M = 12.8 \times 10^6 \text{ g mol}^{-1}$), is again clearly visible. The widths of the distributions are 180 and 890 nm^3 , respectively. The ratio of the weights of the smaller to the larger nanoparticles is about 1:7.

Comparison with Dynamic Light Scattering. The reported mean hydrodynamic radius of Resovist nanoparticles¹⁸ is ~ 30 nm, which is significantly larger than the radii determined by SAXS. Therefore, we collected fractions of the nanoparticles at the SAXS outlet and measured them with DLS. The resulting volume-weighted hydrodynamic radii and the DLS intensities are summarized in Figure 7. It can be seen that the hydrodynamic radii increase from about 5 to 50 nm in the fractionation time interval from 400 to 1800 s. A first weak intensity maximum is visible at approximately $t = 700$ s, which corresponds to $R_h = 15$ nm. An intense second maximum is found at a fractionation time around 1500 s, where R_h is 31 nm. The radius at the intense maximum agrees well with the $R_h = 30$ nm of the nonfractionated Resovist.^{18,26} A comparison of DLS and SAXS data shows the R_h values to be larger than the R values from SAXS at all fractionation times. This is in agreement with the assumption

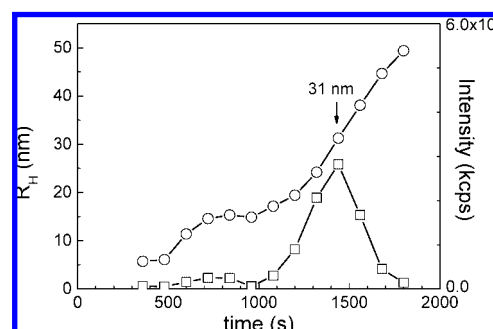


Figure 7. Volume-weighted hydrodynamic radii (circles) and scattering intensities (squares) from dynamic light scattering of Resovist nanoparticles as a function of the fractionation time. The arrow indicates the maximum of the light scattering intensity at a hydrodynamic radius of 31 nm.

that the presence of a polymeric shell contributes significantly to R_h but not to R (the SAXS contribution of the carboxydextran is negligibly small, as already mentioned). We tentatively calculate the thickness of the polymeric shell, R_{shell} , as the difference between R_h and R . Using this assumption, we determined thicknesses of approximately $R_{\text{shell}} = 10$ and 20 nm for the carboxydextran layer of the smaller and larger particle populations, respectively. As a trend, it can be said that the thickness of the shell increases with increasing size of the iron oxide core. The thickness of the shell is not constant, which a priori would also have been a reasonable possibility.

CONCLUSIONS

The online coupling of asymmetric flow field-flow fractionation with small-angle scattering (A4F-SAXS) is a suitable instrument for the characterization of commercial superparamagnetic nanoparticles. The presence of a bimodal size distribution can be quantified with respect to the sizes and frequency of the nanoparticles. In cases in which the separation conditions of the field-flow fractionation are of reasonable quality, the A4F-SAXS could be used as a standard analytical method for characterizing different nanoparticle batches either for scientific research or quality control in commercial production. The time required is ~ 30 min. It must be said that standard X-ray tubes are sufficient for strongly

scattering nanoparticles, such as metals or metal oxides, but intense synchrotron radiation will be required for weak X-ray scatterers, such as proteins and water-soluble polymers.

ACKNOWLEDGMENT

The financial support of the Federal Institute for Materials Research and Testing is gratefully acknowledged. We also thank

H. Schnablegger and R. Bienert for working with the SAXSess and helpful discussions.

Received for review September 22, 2008. Accepted November 5, 2008.

AC802009Q